JOC The Journal of Organic Chemistry

Article

pubs.acs.org/joc

Ultrafast Time Resolved Spectroscopic Studies on the Generation of the Ketyl-Sugar Biradical by Intramolecular Hydrogen Abstraction among Ketoprofen and Purine Nucleoside Dyads

Ming-De Li,[†] Li Dang,*[,‡] Mingyue Liu,[†] Lili Du,[†] Xuming Zheng,[§] and David Lee Phillips*[,†]

[†]Department of Chemistry, The University of Hong Kong, Pokfulam Road, Hong Kong S.A.R., P.R. China

[‡]Department of Chemistry, South University of Science and Technology of China, Shenzhen, Guangdong 518055, China

[§]Department of Chemistry, Zhejiang Sci-Tech University, Hangzhou 310018, China

Supporting Information

ABSTRACT: Intramolecular hydrogen abstraction reactions among ketoprofen (KP) and purine nucleoside dyads have been proposed to form ketyl-sugar biradical intermediates in acetonitrile. Femtosecond transient absorption studies on KP and purine nucleoside dyads reveal that the triplet state of the KP moiety of the dyads with cisoid structure decay faster (due to an intramolecular hydrogen abstraction reaction to produce a ketyl-sugar biradical intermediate) than the triplet state of the KP moiety of the dyads with transoid structure detected in acetonitrile solvent. For the cisoid 5-KP-dG dyad, the triplet state of the KP moiety decays too fast to be observed by ns-TR^3; only the ketyl-sugar biradical intermediates are detected by ns-TR^3 in acetonitrile. For the cisoid 5-KP-dA dyad, the triplet states of the KP moiety could be observed at early nanosecond delay times, and then it quickly undergoes intramolecular hydrogen abstraction to produce a ketyl-sugar biradical intermediate. For the cisoid 5-KPGly-dA and transoid 3-KP-dA dyads, the triplet state of the KP moiety had a longer lifetime due to the long distance chain between the KP moiety and the purine nucleoside (5-KPGly-dA) and the transoid structure (3-KP-dA). The experimental and computational results suggest that the ketyl-sugar biradical intermediate is generated with a higher efficiency for the cisoid dyad. However, the transoid dyad exhibits similar photochemistry behavior as the KP molecule, and no ketyl-sugar biradical intermediate was observed in the ns-TR^3 experiments for the transoid 3-KP-dA dyad.

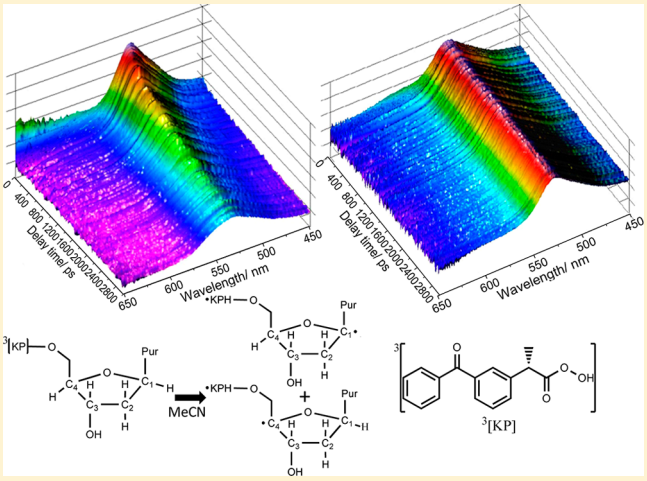

INTRODUCTION

The sequence of heterocyclic bases in double-helical deoxyribonucleic acid (DNA) provides the genetic code that serves as the blueprint for all cellular operations.[1,2] Chemical modification of cellular DNA may greatly influence biological cellular metabolism, induction of DNA repair proteins, inhibition of cell growth, or cell death via either necrotic or apoptotic mechanisms.[3−6] Thus, the study of the agents that damage DNA is of both practical and fundamental importance to diverse fields like medicinal chemistry, carcinogenesis, toxicology, and biotechnology.[7] Oxidative damage to DNA may be induced by a number of agents, such as free radicals, reactive oxygen species (ROS), UV light, or ionizing radiation.[8−11] Researchers have found that the nucleobases and the sugar moiety are the main units to be attacked. Abstraction of hydrogen atoms from the sugar−phosphate backbone typically leads to scission of the DNA chain by complex reaction cascades.[12−16] In addition, there are rather a small number of functional groups or structural motifs that have the ability to lead to efficient modification of cellular DNA.[17−21] Employing photosensitizers to induce and trap the modification of the cellular DNA helps make the detection more convenient and is therefore an attractive area for research.

Ketoprofen (KP) has seen more chemical and biological research recently as it is an important typical Type I photosensitizer.[22−32] A number of studies have been carried out to study the phototoxic and photoallergic reactions induced by KP as well as the interaction between KP and DNA, amino acid, protein to help gauge the safety of KP.[33−39] These studies successfully established the molecular basis for the investigation of phototoxic and photoallergic properties caused by KP. Normally, the formation of DNA single strand breaks is relatively low. However, DNA damage can also result from the absorption of photons by other molecules and photosensitizers. For example, KP at a very low concentration may induce DNA

Received: January 8, 2015
Published: March 3, 2015

DOI: 10.1021/acs.joc.5b00047
J. Org. Chem. 2015, 80, 3462−3470

Scheme 1. Structure of Target Molecules

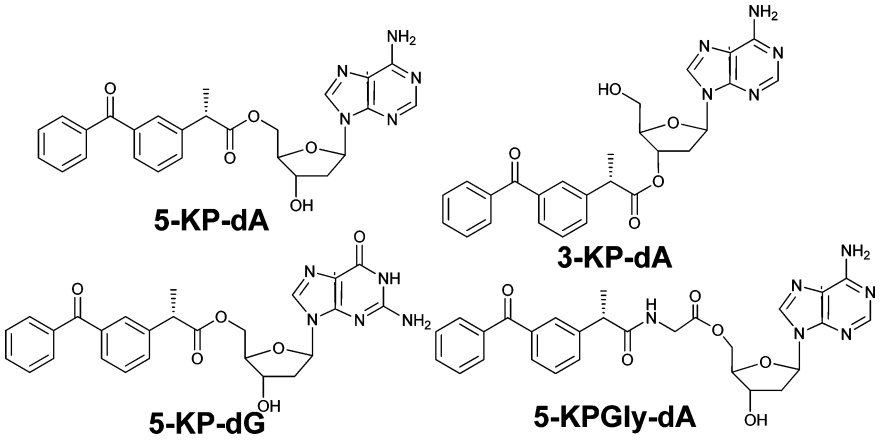

damage in vitro upon irradiation and then photosensitize the formation of pyrimidine dimers and single strand breaks with high quantum yields.[34] The possible mechanism(s) may be related to a substituted benzophenone, which is able to induce both electron and energy transfer to DNA. Similar behaviors have also been observed for DNA damage caused by other NSAIDs.[40] Chouini-Lalanne and co-workers have pointed out that KP undergoes a decarboxylation process, generating radical derivatives and the corresponding photoproducts which damage DNA and stimulate lytic activity on cells when KP is irradiated in aqueous buffer solution.[22]

In order to more fully understand the interaction between DNA and KP, scientists have utilized a single nucleoside as a model to investigate the reaction mechanism(s) between KP and nucleosides.[41] Photosensitization of DNA induced by KP involves two major types of mechanisms: (1) triplet−triplet energy transfer leading to thymine dimerization and (2) an electron-transfer oxidation of the guanine nucleobase.[30,34] Nanosecond laser flash photolysis has been used by Miranda and co-workers to study the possible enantiodifferentiation during DNA nucleosides photosensitization by KP.[42] A significant enantiodifferentiation was observed in the quenching of triplet KP by thymine and deoxyguaosine which can be related to the Pateno−Buchi photoreaction and ketyl radical formation. However, KP photosensitized purine nucleosides have not been widely studied.[43] A better understanding of the photochemical reactivity of a KP photosensitizer toward the DNA nucleobases is essential to anticipate the photobiological risk associated with their use by patients.

At present, the explicit identification of the reaction intermediates and elucidation of the reaction mechanisms of KP and purine nucleoside dyads are still not clear since only a few studies have been done to examine the chemical reactivity relationships and environmental effects on the photosensitization processes. A deeper and more precise knowledge of the active sites and reaction mechanisms can make an important contribution to improve the understanding of the photosensitizing potential of new drug candidates. The rate of the photochemical reaction induced by drugs is always very fast, most of the intermediates generated from the reactions of interest may only last for a very short while and likely on the picosecond or nanosecond time scale. In addition, the complexity of the photochemical reaction process of KP and related drug molecules also makes this type of study difficult. We are pleased to report here a femtosecond transient absorption (fs-TA) and nanosecond time-resolved resonance Raman (ns-TR^3) study of the intramolecular hydrogen abstraction of different KP-purine nucleoside dyads after photolysis. To our knowledge, this is the first ultrafast time-resolved spectroscopic (fs-TA) and time-resolved vibrational spectroscopic (ns-TR^3) investigation of the intramolecular hydrogen abstraction of different KP-purine nucleoside dyads following photoexcitation by ultraviolet light. Results from these new studies provide new experimental data on the ultrafast processes, kinetics and vibrational fingerprint data of reactive intermediates that enable us to gain further insight into the nature of the key reactive intermediates and reaction mechanisms associated with KP photosensitization processes.

RESULTS AND DISCUSSION

KP-purine nucleoside dyads were synthesized according to methods previously reported in the literature.[43] Scheme 1 shows the side chain of KP connected with the deoxyguanosine (dG), deoxyadenosine (dA) and glycine derivative (KPGly) with deoxyadenosine (dA). 5-KP-dA and 3-KP-dA are a couple of compounds with cisoid vs transoid spatial arrangement, 5-KP-dG and 5-KPGly-dA have cisoid configuration like 5-KP-dA.

Intramolecular Hydrogen Abstraction (IHA) among KP and KP Nucleoside Dyads in the MeCN. Figure 1 presents ns-TR^3 spectra of 1 mM 5-KP-dA and 3-KP-dA obtained in acetonitrile (MeCN). Although 5-KP-dA and 3-KP-dA are isomers, the feature of the ns-TR^3 spectra of 5-KP-dA exhibit a noticeable difference from that of 3-KP-dA. For 5-KP-dA, at an early nanosecond delay time (0 ns), the main resonance Raman spectra have bands at 966, 1173, 1222, and 1540 cm^{-1} accompanied by a small band at 1583 cm^{-1}. At later delay times, the first species quickly decays and the band at 1583 cm^{-1} dramatically increases in intensity. However, for 3-KP-dA, the main Raman bands appear at 966, 1173, 1222, and 1540 cm^{-1} and remain visible within 250 ns, only a very weak band at 1583 cm^{-1} is observed. In an attempt to identify the intermediates observed here, the contribution of the second intermediate was removed to obtain a subtracted resonance Raman spectrum at early time (0 ns), which was then compared with an authentic spectrum of the triplet state of KP (^{3}KP) observed in MeCN (this comparison is shown in Figure 2).[25] The excellent correlation between these two spectra demonstrates that the first transient species for 5-KP-dA is the triplet state character species, which is associated with the

DOI: 10.1021/acs.joc.5b00047
J. Org. Chem. 2015, 80, 3462−3470

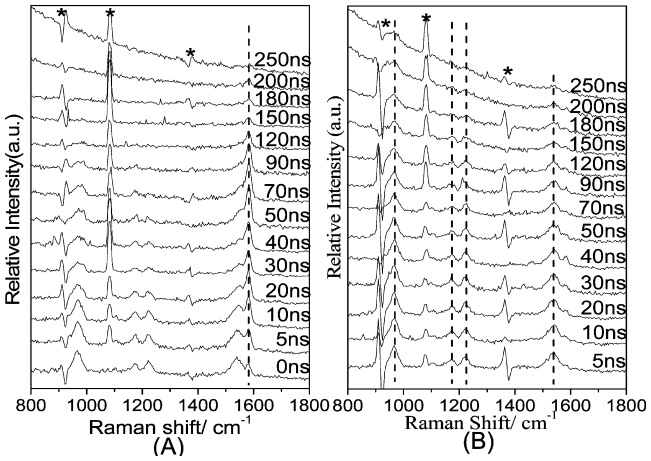

Figure 1. ns-TR^3 spectra of 5-KP-dA (A) and 3-KP-dA (B) recorded in MeCN with various delay times indicated next to the spectra. The asterisks (*) mark subtraction artifacts or laser lines.

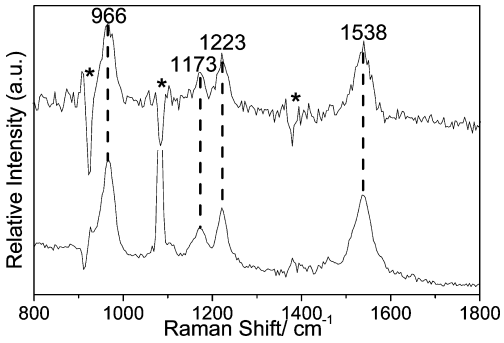

Figure 2. Comparison of the subtracted ns-TR^3 spectrum of 5-KP-dA obtained in MeCN at 0 ns (top) (see text for more details) and the authentic ns-TR^3 spectrum of KP obtained in the MeCN at 0 ns (bottom). The asterisk (*) marks a subtraction artifact or laser line.

chromophore of KP of the 5-KP-dA dyad (represented as 5-^{3}[KP]-dA here). This intermediate promptly produces the second species even in the MeCN solvent. In contrast, the triplet state of 3-KP-dA (3-^{3}[KP]-dA) has a relatively long lifetime, just like the ^{3}KP species formed after photoexcitation of KP in MeCN.

In the following sections, two questions are addressed: (1) Why do these two isomers exhibit very different photochemical behavior? (2) What intermediate is generated at later times for 5-KP-dA? When KP is irradiated by the 266 nm pump laser in MeCN, a weak band is observed that correlates with the decay of ^{3}KP. This weak intermediate could be generated by an intramolecular hydrogen abstraction.[25] As for 3-KP-dA, the analogous feature is also observed. But for 5-KP-dA, the Raman signal of the new species is so large that it overwhelms the Raman intensity of 5-^{3}[KP]-dA. Miranda and co-workers reported that the intramolecular interaction between KP and the purine base resulted in a remarkable quenching of the excited KP-like triplet state.[43] This could in principle be associated with an electron transfer process. To explore the reaction efficiency between the intramolecular interaction and the intermolecular interaction, we also carried out ns-TR^3 experiments of 1 mM KP and 1 mM deoxyguanosine (dA) in an MeCN solvent (see Figure S1, Supporting Information). Inspection of Figure S1 indicates that only the Raman signal of ^{3}KP could be detected, the band at 1583 cm^{-1} is scarcely observed. This demonstrates that the intermolecular interaction of KP and dA cannot efficiently achieve the electron transfer and hydrogen abstraction due to the low collision probability between the free ^{3}KP and dA species, while the intramolecular interaction of 5-KP-dA with a cisoid structure may achieve a high efficiency for the intramolecular hydrogen abstraction. Photolysis of KP-tethered purine nucleosides dyads evolves 2-deoxyribonolactone through the generation of a ketyl-C_1 biradical intermediate.[43] Ns-TR^3 spectra of 5-KP-dA demonstrate that a ketyl-sugar biradical intermediate is probably produced even in the relatively inert solvent (MeCN), which implies water may not be needed for producing the ketyl-sugar biradical intermediate.[43] This reveals that hydrogen bonding may not be necessary for the intramolecular hydrogen abstraction between the KP and purine nucleoside base in the electronic excited state reaction.[44]

However, one may expect that hydrogen bonding and the pH of an aqueous may be able to strongly affect the intramolecular hydrogen abstraction between KP and purine nucleoside base in the electronic excited state reaction. For example, the triplet state of KP can undergo a decarboxylation reaction in aqueous solutions which is consistent with results from density functional theory (DFT) calculations that show as more water molecules become involved in the reaction system the activation energy barriers for the decarboxylation reaction will decrease.[28] These results indicate that water molecules are able to assist excited state intramolecular proton transfer (ESIPT) from the carboxylate group to the carbonyl group, followed by C−C bond cleavage, loss of CO_2 and intramolecular charge transfer so that the triplet protonated biradical carbanion (^{3}BCH) intermediate appears to be directly produced from the neutral form of the triplet KP intermediate by a quick ESIPT and decarboxylation in aqueous solutions.[28] Similarly, varying the pH of an aqueous solution can also significantly influence the decarboxylation reactions of KP so that an acid assisted decarboxylation takes place in strongly acidic aqueous solutions.[28] A recent study of the 2-acetoxymethyl-2-(3-benzoyl-phenyl)-propionic acid (KP-OAc) phototrigger compound found that in neutral high water concentration or acidic aqueous solution this compound will exhibit a water and/or acid assisted photodecarboxylation reaction to directly produce a biradical intermediate that does not cause release of the OAc^- group so that the lifetime of the biradical intermediate of KP-OAc is similar to that of the biradical intermediate produced from KP in the analogous types of solutions.[28,32] In contrast to this, the photodecarboxylation of KP-OAc in a phosphate buffer solution (PBS) directly forms the benzylic carbanion intermediate that can cause the phototrigger reaction to release the OAc^- group so that the lifetime of the biradical intermediate of KP-OAc is much shorter than the lifetime of the biradical intermediate of KP in PBS.[28,32] The preceding results for KP and KP-OAc in aqueous solution[28,32] of varying pH suggests that hydrogen bonding between a solvent like water and the KP-purine dyads may also play a role on the electron transfer and intramolecular hydrogen abstraction reactions and this should be an interesting area of investigation in the future for KP-purine dyads and related systems.

Previous studies found that the triplet states of benzophenone (BP) and KP were efficiently photoreduced by hydrogen atom donors to produce ketyl radical intermediates.[25,45−47] Given the generation of biradical intermediates in the MeCN, an intramolecular hydrogen abstraction process between KP

DOI: 10.1021/acs.joc.5b00047
J. Org. Chem. 2015, 80, 3462−3470

and purine nucleosides is likely involved. In order to study this apparent intramolecular hydrogen abstraction, the same experiments were also carried out for the 5-KP-dG and 5-KPGly-dA systems. The ns-TR^3 spectra of these two dyads are displayed in Figure 3. For the 5-KP-dG dyad, the ns-TR^3

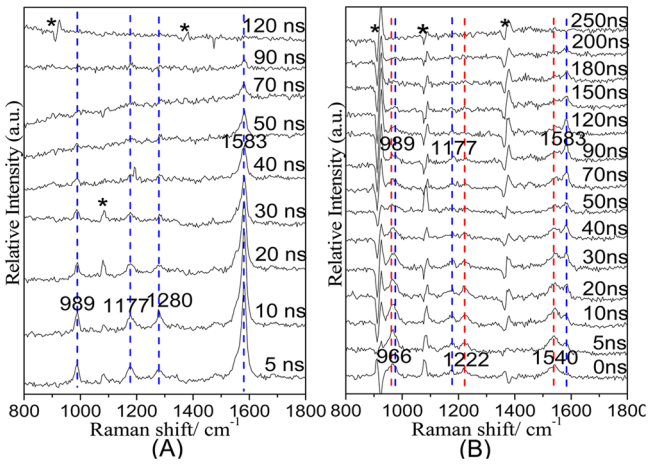

Figure 3. ns-TR^3 spectra of 5-KP-dG (A) and 5-KPGly-dA (B) recorded in MeCN obtained with various delay times indicated next to the spectra. The asterisks (*) mark subtraction artifacts or laser lines.

spectra of the triplet state of 5-KP-dG (5-^{3}[KP]-dG) were not observed using the about 5 ns resolution of the ns-TR^3 instrument. This implies that the more basic guanine may promote the intramolecular hydrogen abstraction so that only the biradical intermediate can be observed in the ns-TR^3 spectra. In contrast, the increase in the length of the distance between the KP and deoxyadenosine, moieties in 5-KPGly-dA causes the lifetime of the triplet state of 5-KPGly-dA (5-^{3}[KPGly]-dA) become a bit longer. These results demonstrate that the more basic site (guanine) appears to accelerate the intramolecular hydrogen abstraction, which is consistent with literature results that guanine is a fragile section with a propensity to be broken in DNA chains when DNA damage was photoinduced by fenofibrate and KP in vitro.[4,40,41] While the elongation of the length between KP and nucleoside dyads will lower the chances for the intramolecular hydrogen abstraction.

Femtosecond Transient Absorption Study of the Dynamics of the Dyads in Acetonitrile. In order to study the kinetics of the apparent intramolecular hydrogen abstraction process for the KP-purine dyads of interest, femtosecond transient absorption (fs-TA) spectroscopy was employed to investigate the early time intermediates generated after irradiation by 267 nm pump laser light. The fs-TA spectra of the 5-KP-dA, 3-KP-dA, 5-KPGly-dA dyads are shown in the Supporting Information and spectra for the 5-KP-dG dyad are shown in Figure 4. For the four dyads, as the maximum absorption band around 335 nm rapidly decreases in intensity and shifts down to a 325 nm band and a weak broad band around 580 nm also drops in intensity, a strong transient absorption band promptly arises at 524 nm on the early picosecond time scale. The bands around 335 and 580 nm are associated with the $S_1 \rightarrow S_n$ transient absorption and the bands around 325 and 524 nm are due to the $T_1 \rightarrow T_n$ transient absorption.[31,48] The decay dynamics of the 335 nm band is almost equal to the growth kinetics of the 524 nm band (see Figure 5 (right)) and this implies that a highly efficient intersystem crossing (ISC) transforms the singlet state to the triplet state for the KP moiety of the dyads. Interestingly, for the 5-KP-dG dyad as the decay of the band at 524 nm occurs, a small shoulder feature around 545 nm begins to emerge and the band at 325 nm increases in intensity and shifts up to 329 nm. The band at 545 nm was assigned to the formation of a ketyl-sugar biradical intermediate in the aqueous solution,[43] and the fs-TA spectra here indicates that the decay of the 5-^{3}[KP]-dG dyad leads to the generation of a ketyl-sugar biradical intermediate by an intramolecular electron-transfer and/or intramolecular hydrogen abstraction mechanism.[49−51]

Figure 5 shows the dynamics of the triplet state for the four dyads examined in our study. These results show that the dynamics of the 3-^{3}[KP]-dA and 5-^{3}[KPGly]-dA dyads are almost same as that of ^{3}KP that do not decay significantly within 3 ns and this is also consistent with the triplet state of these two dyads being readily detected in the ns-TR^3 experiments detailed in the previous section. The decay rate of the 5-^{3}[KP]-dA dyad with the cisoid structure is observed to be somewhat faster than that of the 3-^{3}[KP]-dA dyad with the transoid structure. The 5-^{3}[KP]-dG dyad species exhibits the fastest decay in intensity compared with the other three dyads. Figure 5 (right) shows plots of the four exponential best-fits to the experimental data points at 330 and 524 nm. The time constants determined from these fits are τ_1 = 0.26 ps, τ_2 = 7.4 ps, τ_3 = 110 ps and τ_4 = 1.5 ns and τ_1 = 0.26 ps, τ_2 = 7.2 ps, τ_3 = 111 ps and τ_4 = 1.7 ns for 330 and 524 nm, respectively. τ_1 = 0.26 ps is associated with internal conversion (IC) from S_n to S_1. τ_2 = 7.2−7.4 ps is associated with intersystem crossing (ISC) transformation from S_1 to T_1(n, π^*) and this time constant is faster than that of benzophenone (10 ps) obtained

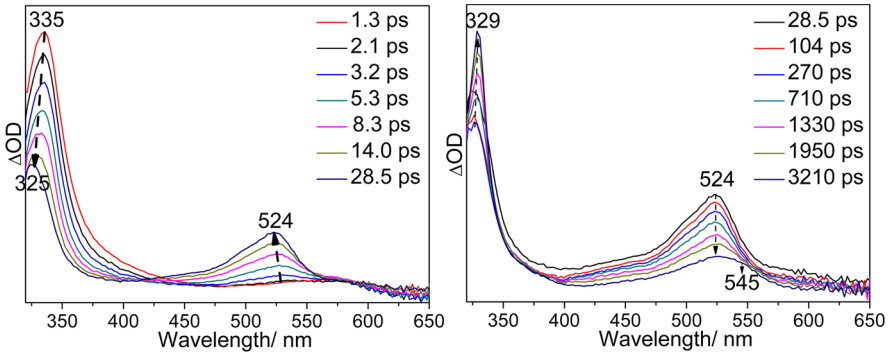

Figure 4. Femtosecond transient absorption spectra of 5-KP-dG at various delay times after photoexcitation at 267 nm in MeCN.

DOI: 10.1021/acs.joc.5b00047
J. Org. Chem. 2015, 80, 3462−3470

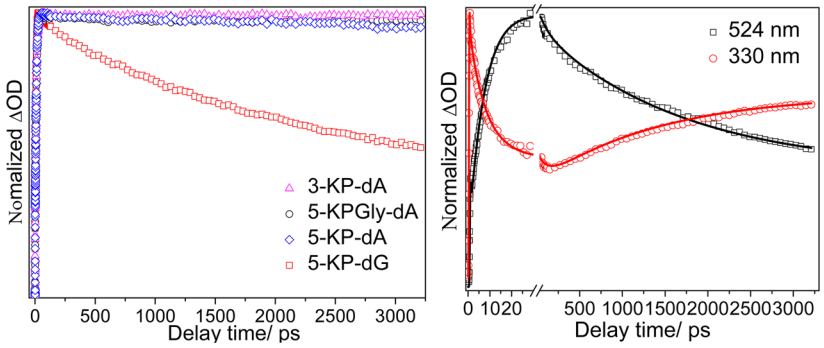

Figure 5. Temporal dependence of the normalized transient absorption intensity of the four dyads recorded at 524 nm in MeCN solvent are shown. (right) Temporal dependence of the normalized transient absorption intensity for 5-KP-dG recorded at 524 and 330 nm in MeCN are shown. Solid lines indicate kinetics fitting using a four exponential function to fit the experimental data points.

in MeCN. τ_3 = 110 ps is the lifetime of the electron transfer from deoxyguanosine to KP and τ_4 = 1.5−1.7 ns is the time constant of the intramolecular hydrogen abstraction reaction. This means that the lifetime of 5-^{3}[KP]-dG is about 1.6 ns which cannot be easily observed in the about 5 to 10 ns resolution of ns-TR^3 experiments. Therefore, the 5-^{3}[KP]-dG species was not explicitly observed by ns-TR^3 spectra for this dyad as the hydrogen abstraction process was faster than the resolution of the ns-TR^3 experiments. The results of fs-TA experiments correlate with the results observed by ns-TR^3 experiments in MeCN.

DFT Study on Intramolecular Hydrogen Abstraction among Dyads. In an attempt to shed more light on the mechanism of the formation of the ketyl-sugar biradical intermediate, density functional theory (DFT) calculations were performed to calculate the structures and properties of the intermediates involved in the intramolecular hydrogen abstraction reaction of interest. These results reveal that the ring of the sugar moiety of 5-^{3}[KP]-dA is parallel with the carbonyl group of the KP chromophore, while the ring of the sugar moiety of 3-^{3}[KP]-dA lies a lower position than does the carbonyl group of the KP chromophore (see a depiction of these structures in Figure 6). Rotation of the dihedral angle

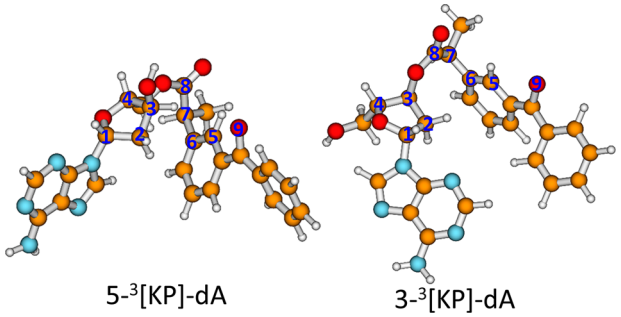

Figure 6. Simple depictions of the optimized structures of 5-^{3}[KP]-dA and 3-^{3}[KP]-dA intermediates obtained from B3LYP/6-31G* DFT calculations. See text and Supporting Information for more details.

among $C_5-C_6-C_7-C_8$, the p orbital of O_9 will become very close to the hydrogen atoms of C_2 and C_3 in the sugar ring of the 5-^{3}[KP]-dA dyad species, thus making the hydrogen atom transfer from C_2 or C_3 to carbonyl group of the KP chromophore conveniently. However, for 3-^{3}[KP]-dA, the p orbital of O_9 could not reach the hydrogen atom of the sugar moiety because of its transoid structure and steric effects.

Previous studies showed that the n, π^* ^{3}KP species has a strong ability to abstract a hydrogen atom from a hydrogen donor.[25] Practically, the n, π^* ^{3}KP species could also undergo a process with a weak hydrogen donor (H_2O) to produce a ketyl radical species.[24,25] By the same way, the ^{3}KP moiety of the dyad may probably abstract a hydrogen atom from C_2 and C_3 positions of the sugar in 5-^{3}[KP]-dA dyad species to generate ketyl-C_2 and/or ketyl-C_3 biradical intermediates. Figure S5 describes the optimized process of intramolecular hydrogen abstraction. After the rotation of the dihedral angle of $C_5-C_6-C_7-C_8$, the hydrogen atom at the C_2 and C_3 positions are able to access the C═O group between the two benzene rings. The C═O bond length is 1.328 for both 5-^{3}[KP]-dA and 5-^{3}[KP]-dG, which demonstrates that the ^{3}KP in the dyads are in a typical n, π^* triplet state. The active center of the triplet state dyads is located on the C═O groups. Thus, C═O may abstract a hydrogen atom from C_2 and C_3 positions of the sugar ring in 5-^{3}[KP]-dA and 5-^{3}[KP]-dG.

Figure 7 shows the energy profiles of the intramolecular hydrogen abstraction from the C_2 and C_3 positions of the

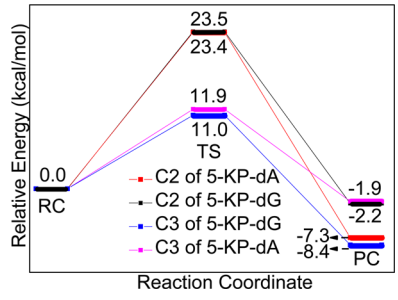

Figure 7. Energy profiles in the MeCN solvent for the intramolecular hydrogen abstraction reactions at the C_2 and C_3 position in the 5-KP-dA and 5-KP-dG dyads. The relative free energies are given in kcal/mol. See text and Supporting Information for details.

sugars in 5-KP-dA and 5-KP-dG dyads. The energy barriers for the abstraction hydrogen from C_2 of sugar in the 5-^{3}[KP]-dA and 5-^{3}[KP]-dG dyads are 23.4 and 23.5 kcal/mol respectively, which are higher than that of abstraction hydrogen from C_3 of sugar in the 5-^{3}[KP]-dA and 5-^{3}[KP]-dG dyads by 11.5 and 12.5 kcal/mol. However, on one hand, the free energy of diradical products with C_2 radical for 5-KP-dG dyad and diradical products with C_3 radical for 5-KP-dA dyad are a little stable than that of the reactants (RC) by 1.9 and 2.2 kcal/mol in 5-^{3}[KP]-dA and 5-^{3}[KP]-dG dyads, suggesting that there is

DOI: 10.1021/acs.joc.5b00047
J. Org. Chem. 2015, 80, 3462−3470

an equilibrium between the reactants and the diradical products. On the other hand, the diradical products with C_2 radical for 5-KP-dA dyad and diradical products with C_3 radicals for 5-KP-dG dyad are more stable than that of the reactants (RC) by 7.3 and 8.4 kcal/mol in 5-^{3}[KP]-dA and 5-^{3}[KP]-dG dyads respectively, suggesting that the formation of these diradical products is irreversible. However, the relative energy barrier (11.0 kcal/mol) of the intramolecular hydrogen abstraction reactions at the C_3 of sugar in the 5-^{3}[KP]-dG dyad is lower than that (23.4 kcal/mol) of the intramolecular hydrogen abstraction reactions at the C_2 of sugar in the 5-^{3}[KP]-dA dyad. This suggests that the triplet state of KP moiety of 5-^{3}[KP]-dG dyad is easier and faster to be consumed than that of 5-^{3}[KP]-dA dyad. These calculated results could reasonably explain the experimental observation that the 5-^{3}[KP]-dG intermediate decays faster than the 5-^{3}[KP]-dA intermediate does and also the 5-^{3}[KP]-dG transient could not be detected in the ns-TR^3 experiments whereas the 5-^{3}[KP]-dA transient could be detected at early nanosecond times in the ns-TR^3 experiments under the same conditions. On the basis of these calculated results, the hydrogen atoms of C_2 and C_3 are all possible to be captured by the oxygen of the C═O group of the triplet state cisoid dyads.

The reaction barriers for the hydrogen abstraction typically correlate with the C−H bond strength. The C−H bond enthalpies calculated for abstraction of hydrogen from the C_1, C_2, C_3 and C_4 positions of the deoxyribose sugar moiety reveal similar C−H bond strengths for the C_1, C_3 and C_4. In these cases, the resulting carbon-centered radicals are stabilized by the adjacent oxygen.[52] Table 1 shows the relative energies to form a radical at the sugar C_1, C_2, C_3 and C_4 positions for the 5-KP-dA and 5-KP-dG dyads. Although the hydrogen atom at the C_2 and C_3 positions are easy to be abstracted by the carbonyl group (O_9), the radicals at the C_2 and C_3 positions possess higher free energies compared with the ones at the other two positions. Especially the free energy of the radical at the C_1 position is dramatically lower than that of the radical at the C_2 position. Our calculation results are reasonably consistent with the relative stability of the different sugar radicals that have been calculated by several other groups,[53−58] and the order is generally found to be $C_1 > C_4 > C_5 > C_3 > C_2$. The lower energy levels of the sugar radicals at C_1 and C_4 positions drive the radicals at the C_2 and C_3 positions to further isomerize to the C_1 and C_4 positions respectively through a hydrogen shift. As a consequence, the radicals at the C_1 and C_4 positions are very stable and should be predominant after reaching equilibrium. Kumar and co-workers also reported that for the neutral sugar radicals of 2′-deoxyguanosine, C_1 has the lowest vertical ionization potential, ca. 6.33 eV in the gas phase. C_2 has the highest vertical ionization potential, ca. 8.02 eV in the gas phase, and the resultant C_2 cation is predicted to undergo a barrierless hydride transfer from the C_2 site to produce the C_1 cation.[59]

Table 1. Relative Free Energies in the MeCN Solvent Required to Generate a Biradical at the C_1, C_2, C_3 and C_4 Positions for Sugar in the 5-KP-dA and 5-KP-dG Dyads Compared to RC

		carbon positions			
relative free energies, kcal/mol	RC	C_1	C_2	C_3	C_4
5-KP-dA	0.0	−15.6	−7.3	−1.9	−16.2
5-KP-dG	0.0	−9.6	−2.2	−8.4	−12.2

Among the four dyads, after irradiation the strongest ns-TR^3 spectra were recorded for the 5-KP-dG intermediates compared to other dyads. Therefore, the 5-KP-dG system is used as model to ascertain the assignment of the transient species and the vibrational frequencies. Figure 8 shows the comparison of the ns-TR^3 spectrum of 5-KP-dG obtained in MeCN at 10 ns and the calculated predicted normal Raman spectrum of the biradical intermediates with one radical at the C_1 and C_4 positions in the sugar ring for 5-KP-dG. The excellent agreement between these spectra indicates that the intermediates observed in MeCN for the 5-KP-dG and 5-KP-dA can be assigned to the ketyl-C_1 biradical and ketyl-C_4 biradical species. In several other studies, the C_1 sugar radical formation was also observed predominantly.[60−65] Shukla and co-workers also proposed that one-electron oxidized guanine will form the C_1 sugar radical and another sugar radical at the C_3 or C_4 positions from visible and UV photolysis.[66] The observation of the final 2-deoxyribonolactone (dL) also demonstrated that a ketyl-C_1 biradical intermediate was generated after irradiation of 5-KP-dG in the presence of oxygen.[43] This may support the abstraction of the hydrogen at C_2 position as an initial step by an intramolecular hydrogen abstraction in the relatively inert MeCN solvent and subsequently the radical is inclined to transfer to the C_1 position at a lower energy level. Eventually, the ketyl-C_1 biradical intermediate could react with the oxygen dissolved in the solvent and generate 5-KP-dL product.[43] TD-DFT calculations were also performed to further characterize the 5-KP-dL species. These calculation results show that 5-KP-dL has strong oscillator strengths at 185 and 261 nm. The higher oscillator strength at 185 nm is mainly contributed from the sugar chromophore while another low one at 261 nm is associated with the KP chromophore. Figure S6 shows the calculated predicted UV−vis absorption of 5-KP-dL. Therefore, when 319.9 nm was used as the probe wavelength in the ns-TR^3 experiments, it is very hard to acquire the resonance Raman spectra of the final product due to the deep ultraviolet absorption of the sugar moiety.

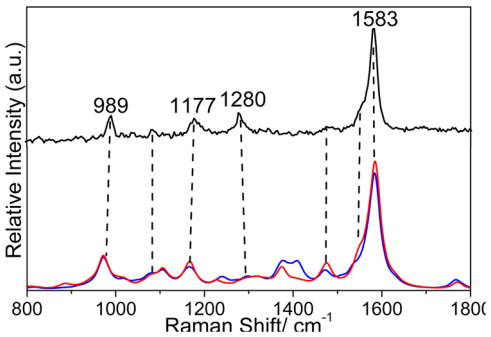

Figure 8. The comparison of the ns-TR^3 spectrum of 5-KP-dG obtained in MeCN at 10 ns (black) and the calculated predicted normal Raman spectra of the biradical intermediates with the radical at the C_1 (blue) and C_4 (red) positions in the sugar ring for 5-KP-dG (bottom).

CONCLUSIONS

In conclusion, a combined experimental/computational study has provided more insight into the photochemical mechanism for the generation of ketyl-sugar biradical intermediates among

DOI: 10.1021/acs.joc.5b00047
J. Org. Chem. 2015, 80, 3462−3470

KP-Purine dyads (Scheme 2), where intramolecular hydrogen abstraction initiated by the triplet state of the KP moiety leads

Scheme 2. Proposed Photochemical Mechanisms of the KP-Purine Dyads in MeCN Based on Results from Our Present Study

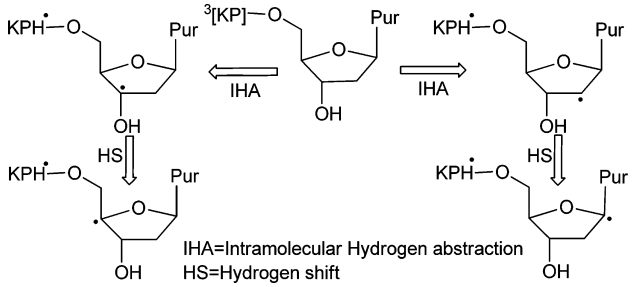

to the ketyl-C_2 and ketyl-C_3 biradical species due to the accessibility of the carbonyl group to the hydrogen atoms that are initially abstracted. Both experimental and computational results show that intramolecular hydrogen abstraction for the cisoid dyads (5-KP-dA and 5-KP-dG) is favorable in MeCN. However, the intramolecular hydrogen abstraction is hindered by the long distance chain for the 5-KPGly-dA system and steric effect for the transoid structure 3-KP-dA. Therefore, 5-KPGly-dA and 3-KP-dA show similar photochemistry behavior as KP in the MeCN solvent. Ketyl-sugar biradical species was not obviously observed in the ns-TR^3 experiments for 5-KPGly-dA and 3-KP-dA. The kinetics data obtained from fs-TA experiments in MeCN also provide direct evidence for a slight decay for the 5-^{3}[KPGly]-dA and 3-^{3}[KP]-dA intermediates relative to the fast decay for the 5-^{3}[KP]-dA and 5-^{3}[KP]-dG triplet state cisoid dyads. DFT calculations studies support that the ketyl-C_2 and ketyl-C_3 biradicals are first formed and then produce the lower energy level ketyl-C_1 and ketyl-C_4 biradical via the radical transferring from the C_2 position to the C_1 position and from the C_3 position to the C_4 position through hydrogen shift processes. Eventually the ketyl-C_1 and ketyl-C_4 biradical are generated for KP-purine dyads in MeCN solvent. Given the recent interest in DNA damage and repair reactions, we believe the current analysis of the intramolecular hydrogen abstraction between the photosensitive KP moiety and purine nucleoside moiety in the dyads examined will help encourage further work into cases where more complicated mechanisms may be encountered. Furthermore, clear characterization of the reaction intermediates and an increased understanding of the reaction mechanisms may also help other researchers in how to best utilize these types of benzophenone derivative drugs and to design improved benzophenone derivative drugs for particular applications with lower photoxicity.

EXPERIMENTAL AND COMPUTATIONAL METHODS

The four KP-purine nucleoside dyads (5-KP-dA, 3-KP-dA, 5-KP-dG and 5-KPGly-dA) used in this study were synthesized according to methods previously reported in the literature.[43] The ^{1}H NMR spectra of these four dyad samples are provided in the Supporting Information. The purity of the four KP-purine dyads were estimated to be ≥98%. The spectroscopic properties of the samples are in full accord with the literature reported spectra.[43]

fs-TA Experiments. The fs-TA experiments were done employing an experimental setup and methods detailed previously[31] and only a brief description is provided here. The fs-TA measurements were done using a femtosecond regenerative amplified Ti:sapphire laser system in which the amplifier was seeded with the 120 fs laser pulses from an oscillator laser system. The laser probe pulse was produced by utilizing ∼5% of the amplified 800 nm laser pulses to generate a white-light continuum (350−800 nm) in a CaF_2 crystal and then this probe beam was split into two parts before traversing the sample. One probe laser beam went through the sample while the other probe laser beam went to the reference spectrometer in order to monitor the fluctuations in the probe beam intensity. For the present experiments, the sample solution was excited by a 267 nm pump beam (the third harmonic of the fundamental 800 nm from the regenerative amplifier). The 40 mL sample solutions were studied in a flowing 2 mm path-length cuvette with an absorbance of 1 at 267 nm throughout the data acquisition.

ns-TR^3 Experiments. The ns-TR^3 experiments were done using an experimental apparatus and methods discussed in detail previously,[28] so only a short description will be given here. The 266 nm pump laser pulse generated from the fourth harmonic of a Nd:YAG nanosecond pulsed laser and a 319.9 nm probe laser pulse generated from the third anti-Stokes hydrogen Raman shift laser line from the second harmonic were used in the ns-TR^3 experiments. The energy for the pump and probe pulses were in the range of 2.5−3.5 mJ with a 10 Hz repetition rate. The two Nd:YAG lasers were synchronized electronically by a pulse delay generator to control the delay time of the pump and probe lasers with the delay time between the laser pulses monitored by a fast photodiode and 500 MHz oscilloscope and the time resolution for the ns-TR^3 experiments was approximately 10 ns. The pump and probe laser beams were lightly focused onto the flowing sampling system and the Raman light was collected using reflective optics into a spectrometer whose grating dispersed the light onto a liquid nitrogen cooled CCD detector. The Raman signal was accumulated for 30 s by the CCD before being read out to an interfaced PC computer and 10−20 scans of the signal were added together to get a resonance Raman spectrum. The ns-TR^3 spectra presented here were obtained by the subtraction of a resonance Raman spectrum with negative delay time of −100 ns (probe-before-pump spectrum) from the resonance Raman spectrum with a positive delay time (pump−probe spectrum) and the Raman shifts were calibrated by the known MeCN solvent Raman bands with an estimated accuracy of 5 cm^{-1}.

DFT Calculations. Density functional theory (DFT) computations were used to investigate the structure and properties of the likely intermediates generated after irradiation of KP-Purine dyads in acetonitrile solvent. The optimized geometries, vibrational modes and the vibrational frequencies for the different species were obtained from (U)B3LYP DFT calculations employing a 6-31G* basis set in PCM solvent model. No imaginary frequency modes were observed at the stationary states of the optimized structures shown here. All of the reactions have been explored by optimizing the structures of the reactant (RC), transition states (TS) and product complexes (PC). Transition states were located using the Berny algorithm. Frequency calculations at the same level of theory have also been performed to identify all of the stationary points as minima for transition states (one imaginary frequency). Intrinsic reaction coordinates (IRC)[67] were calculated for the transition states to confirm that the relevant structures connect the two relevant minima. The Raman spectra were obtained using the default G03 method that used determination of Raman intensities from transition polarizabilities calculated by numerical differentiation, with assumed zero excitation frequency (e.g., using the Placzek approximation). The calculated Raman frequencies from the UB3LYP/6-311G** computations were scaled by a factor of 0.975 to compare with the experimental Raman results in order to make vibrational assignments. All of the calculations were done using the Gaussian 03 program suite.[68]

ASSOCIATED CONTENT

Supporting Information

The fs-TA spectra of the four dyads obtained in acetonitrile, the optimized geometries of RC, TS and PC of 5-^{3}[KP]-dA and 5-^{3}[KP]-dG dyads, DT-DFT calculation predicted the UV−vis absorption of 5-KP-dL, 1H NMR spectra of four dyads and

DOI: 10.1021/acs.joc.5b00047
J. Org. Chem. 2015, 80, 3462−3470

Cartesian coordinates, total energies, and vibrational zero-point energies for the optimized geometry from the (U)B3LYP/6-311G** calculations for the compounds and intermediates considered in this paper are given. This material is available free of charge via the Internet at http://pubs.acs.org.

AUTHOR INFORMATION

Corresponding Authors

*Phone: 852-2859-2160. Fax: 852-2857-1586. E-mail: dang.l@sustc.edu.cn

*Phone: 852-2859-2160. Fax: 852-2857-1586. E-mail: phillips@hku.hk.

Notes

The authors declare no competing financial interest.

ACKNOWLEDGMENTS

We thank Professor Xin-quan Hu at Zhejiang University of Technology for the synthesis of the four ketoprofen-purine dyad compounds (5-KP-dA, 3-KP-dA, 5-KP-dG and 5-KPGly-dA) used in this study. This work was supported by a grant from the Research Grants Council of Hong Kong (HKU 7035/13P) and the University Grants Committee Special Equipment Grant (SEG-HKU-07) to DLP. Partial support from the Grants Committee Areas of Excellence Scheme (AoE/P-03/08) is also gratefully acknowledged.

REFERENCES

(1) Watson, J. D.; Crick, F. H. C. *Nature* **1953**, *171*, 737−738.

(2) Alberts, B.; Johnson, A.; Lewis, J.; Raff, M.; Roberts, K.; Walter, P. *Molecular Biology of the Cell*, 4th ed.; Garland Science: New York, 2002.

(3) Zhou, B. B. S.; Elledge, S. J. *Nature* **2000**, *408*, 433−439.

(4) Rouse, J.; Jackson, S. P. *Science* **2002**, *297*, 547−551.

(5) Green, D. R. *Cell* **2005**, *121*, 671−674.

(6) Norbury, C. J.; Hickson, I. D. *Annu. Rev. Pharmacol. Toxicol.* **2001**, *41*, 367−401.

(7) Gates, K. S. *The Chemical Reactions of DNA Damage and Degradation*; Wiley-Interscience: Hoboken, NJ, 2007.

(8) Chatgilialoglu, C.; O'Neill, P. *Exp. Gerontol.* **2001**, *36*, 1459−1471.

(9) Cadet, J.; Berger, M.; Douki, T.; Morin, B.; Raoul, S.; Ravanat, J. L.; Spinelli, S. *Biol. Chem.* **1997**, *387*, 1275−1286.

(10) Burrows, C.; Muller, J. G. *Chem. Rev.* **1998**, *98*, 1109−1151.

(11) Armitage, B. *Chem. Rev.* **1998**, *98*, 1171−1200.

(12) Breen, A. P.; Murphy, J. A. *Free Radical Biol. Med.* **1995**, *18*, 1033−1077.

(13) Greenberg, M. M. *Chem. Res. Toxicol.* **1998**, *11*, 1235−1248.

(14) Pogozelski, W. K.; Tullius, T. D. *Chem. Rev.* **1998**, *98*, 1089−1108.

(15) Pratviel, G.; Bernadou, J.; Meunier, B. *Angew. Chem., Int. Ed.* **1995**, *34*, 746−769.

(16) Sonntag, C. V.; Hagen, U.; Schon-Bopp, A.; Schulte-Frohlinde, D. *Adv. Radiat. Biol.* **1981**, *9*, 109−142.

(17) Gates, K. S. Covalent modification of DNA by natural products. In *Comprehensive Natural Products Chemistry*; Kool, E. T., Ed.; Pergamon: New York, 1999; Vol. 7, p 491.

(18) Hurley, L. H. *Nat. Rev. Cancer* **2002**, *2*, 188−200.

(19) Wolkenberg, S. E.; Boger, D. L. *Chem. Rev.* **2002**, *102*, 2477−2496.

(20) Remers, W. A. Antineoplastic Agents. In *Textbook of Organic, Medicinal and Pharmaceutical Chemistry*; Lippincott: Philadelphia, PA, 1991.

(21) Lawley, P. D.; Phillips, D. H. *Mutat. Res.* **1996**, *355*, 13−40.

(22) Bagheri, H.; Lhiaubet, V.; Montastruc, J. L.; Louis-Lalanne, N. *Drug Saf.* **2000**, *22*, 339−349.

(23) Martinez, L. J.; Scaiano, J. C. *J. Am. Chem. Soc.* **1997**, *119*, 11066−11070.

(24) Li, M. D.; Du, Y.; Chuang, Y. P.; Xue, J.; Phillips, D. L. *Phys. Chem. Chem. Phys.* **2010**, *12*, 4800−4808.

(25) Chuang, Y. P.; Xue, J.; Du, Y.; Li, M. D.; An, H. Y.; Phillips, D. L. *J. Phys. Chem. B* **2009**, *113*, 10530−10539.

(26) Cosa, G.; Martinez, L. J.; Scaiano, J. C. *Phys. Chem. Chem. Phys.* **1999**, *1*, 3533−3537.

(27) Monti, S.; Sortino, S.; Guidi, G. D.; Marconi, G. *J. Chem. Soc., Faraday Trans.* **1997**, *93*, 2269−2274.

(28) Li, M. D.; Yeung, C. S.; Guan, X.; Ma, J.; Li, W.; Ma, C.; Phillips, D. L. *Chem.—Eur. J.* **2011**, *17*, 10935−10950.

(29) Cosa, G.; Lukeman, M.; Scaiano, J. C. *Acc. Chem. Res.* **2009**, *42*, 599−607.

(30) Lhiaubet, V.; Paillous, N.; Chouini-Lalanne, N. *Photochem. Photobiol.* **2001**, *74*, 670−678.

(31) Li, M. D.; Ma, J.; Su, T.; Liu, M.; Yu, L.; Phillips, D. L. *J. Phys. Chem. B* **2012**, *116*, 5882−5887.

(32) Li, M. D.; Su, T.; Ma, J.; Liu, M.; Liu, H.; Li, X.; Phillips, D. L. *Chem.—Eur. J.* **2013**, *19*, 11241−11250.

(33) Galian, R. E.; Pastor-Prez, L.; Miranda, M. A.; Prez-Prieto, J. *Chem.—Eur. J.* **2005**, *11*, 3443−3448.

(34) Chouini-Lalanne, N.; Defais, M.; Paillous, N. *Biochem. Pharmacol.* **1998**, *55*, 441−446.

(35) Monti, S.; Manet, I.; Manoli, F.; Morrone, R.; Nicolosi, G.; Sortino, S. *Photochem. Photobiol.* **2006**, *82*, 13−19.

(36) Monti, S.; Manet, I.; Manoli, F.; Sortino, S. *Photochem. Photobiol. Sci.* **2007**, *6*, 462−470.

(37) Vaya, I.; Lhiaubet-Vallet, V.; Jimenez, M. C.; Miranda, M. A. *Chem. Soc. Rev.* **2014**, *43*, 4102−4122.

(38) Suzuki, T.; Shinoda, M.; Osanai, Y.; Isozaki, T. *J. Phys. Chem. B* **2013**, *117*, 9662−9668.

(39) Shinoda, M.; Isozaki, T.; Suzuki, T. *Photochem. Photobiol.* **2014**, *90*, 92−98.

(40) Marguery, M. C.; Chouini-Lalanne, N.; Ader, J. C.; Paillous, N. *Photochem. Photobiol.* **1998**, *68*, 679−684.

(41) Lhiaubet-Vallet, V.; Belmadoui, N.; Climent, M. J.; Miranda, M. A. *J. Phys. Chem. B* **2007**, *111*, 8277−8282.

(42) Lhiaubet-Vallet, V.; Encinas, S.; Miranda, M. A. *J. Am. Chem. Soc.* **2005**, *127*, 12774−12775.

(43) Paris, C.; Encinas, S.; Belmadoui, N.; Climent, M. J.; Miranda, M. A. *Org. Lett.* **2008**, *10*, 4409−4412.

(44) Zhao, G. J.; Han, K. L. *Acc. Chem. Res.* **2012**, *45*, 404−413.

(45) Tahara, T.; Hamaguchi, H.; Tasumi, M. *Chem. Phys. Lett.* **1988**, *152*, 135−139.

(46) Yabumoto, S.; Sato, S.; Hamaguchi, H. *Chem. Phys. Lett.* **2005**, *416*, 100−103.

(47) Du, Y.; Ma, C.; Kwok, W. M.; Xue, J.; Phillips, D. L. *J. Org. Chem.* **2007**, *72*, 7148−7156.

(48) Aloise, S.; Ruckebusch, C.; Blanchet, L.; Rehault, J.; Buntinx, G.; Huvenne, J. P. *J. Phys. Chem. A* **2008**, *112*, 224−231.

(49) Chatgilialoglu, C.; Ferreri, C.; Bazzanini, R.; Guerra, M.; Choi, S. Y.; Emanuel, C. J.; Horner, J. H.; Newcomb, M. *J. Am. Chem. Soc.* **2000**, *122*, 9525−9533.

(50) Kumar, A.; Sevilla, M. D. *J. Phys. Chem. B* **2009**, *113*, 13374−13380.

(51) Abad, S.; Bosca, F.; Domingo, L. R.; Gil, S.; Pischel, U.; Miranda, M. A. *J. Am. Chem. Soc.* **2007**, *129*, 7407−7420.

(52) Miaskiewicz, K.; Osman, R. *J. Am. Chem. Soc.* **1994**, *116*, 232−238.

(53) Sarma, R. L.; Medhi, C. *J. Mol. Struct.* **2006**, *763*, 51−57.

(54) Colson, A. O.; Sevilla, M. D. *J. Phys. Chem.* **1995**, *99*, 3867−3874.

(55) Miaskiewicz, K.; Osman, R. *J. Am. Chem. Soc.* **1994**, *116*, 232−238.

(56) Li, M. J.; Liu, L.; Wei, K.; Fu, Y.; Guo, Q. X. *J. Phys. Chem. B* **2006**, *110*, 13582−13589.

(57) Li, M. J.; Liu, L.; Fu, Y.; Guo, Q. X. *J. Phys. Chem. B* **2005**, *109*, 13818−13826.

DOI: 10.1021/acs.joc.5b00047
J. Org. Chem. 2015, 80, 3462−3470

(58) Abolfath, R. M.; van Duin, A. C. T.; Brabec, T. *J. Phys. Chem. A* **2011**, *115*, 11045−11049.
(59) Kumar, A.; Pottiboyina, V.; Sevilla, M. D. *J. Phys. Chem. B* **2012**, *116*, 9409−9416.
(60) Roginskaya, M.; Bernhard, W. A.; Marion, R. T.; Razskazovskiy, Y. *Radiat. Res.* **2005**, *163*, 85−89.
(61) Roginskaya, M.; Razskazovskiy, Y.; Bernhard, W. A. *Angew. Chem., Int. Ed.* **2005**, *44*, 6210−6213.
(62) Xue, L.; Greenberg, M. M. *Angew. Chem., Int. Ed.* **2007**, *46*, 561−564.
(63) Sato, K.; Greenberg, M. E. *J. Am. Chem. Soc.* **2005**, *127*, 2806−2807.
(64) Dedon, P. C. *Chem. Res. Toxicol.* **2008**, *21*, 206−219.
(65) Chen, B.; Zhou, X.; Taghizadeh, K.; Chen, J.; Stubbe, J.; Dedon, P. C. *Chem. Res. Toxicol.* **2007**, *20*, 1701−1708.
(66) Shukla, L. I.; Pazdro, R.; Huang, J.; DeVreugd, C.; Becker, D.; Sevilla, M. D. *Radiat. Res.* **2004**, *161*, 582−590.
(67) Cances, E.; Mennucci, B.; Tomasi, J. *J. Chem. Phys.* **1997**, *107*, 3032−3041.
(68) Frisch, M. J.; Trucks, G. W.; Schlegel, H. B.; Scuseria, G. E.; Robb, M. A.; Cheeseman, J. R.; Montgomery,J. A.; Kudin, T. V., Jr. K, N.; Burant, J. C.; Millam, J. M.; Iyengar, S. S.; Tomasi, J.; Barone, V.; Mennucci, B.; Cossi, M.; Scalmani, G.; Rega, N.; Petersson, G. A.; Nakatsuji, H.; Hada, M.; Ehara, M.; Toyota, K.; Fukuda, R.; Hasegawa, J.; Ishida, M.; Nakajima, T.; Honda, Y.; Kitao, O.; Nakai, H.; Klene, M.; Li, X.; Knox, J. E.; Hratchian, H. P.; Cross, J. B.; Bakken, V.; Adamo, C.; Jaramillo, J.; Gomperts, R.; Stratmann, R. E.; Yazyev, O.; Austin, A. J.; Cammi, R.; Pomelli, C.; Ochterski, J. W.; Ayala, P. Y.; Morokuma, K.; Voth, G. A.; Salvador, P.; Dannenberg, J. J.; Zakrzewski, V. G.; Dapprich, S.; Daniels, A. D.; Strain, M. C.; Farkas, O.; Malick, D. K.; Rabuck, A. D.; Raghavachari, K.; Foresman, J. B.; Ortiz, J. V.; Cui, Q.; Baboul, A. G.; Clifford, S.; Cioslowski, J.; Stefanov, B. B.; Liu, G.; Liashenko, A.; Piskorz, P.; Komaromi, I.; Martin, R. L.; Fox, D. L.; Keith, T.; Al-Laham, M. A.; Peng, C. Y.; Nanayakkara, A.; Challacombe, M.; Gill, P. M. W.; Johnson, B.; Chen, W.; Wong, M. W.; Gonzalez, C.; Pople, J. A. *Gaussian 03*, Revision C.02; Gaussian, Inc.: Pittsburgh, PA, 2004.

DOI: 10.1021/acs.joc.5b00047
J. Org. Chem. 2015, 80, 3462−3470